Research Article

Pyrolysis of Polyethylene from Plastic Waste using Activated Ende Natural Zeolite as a Catalyst

Gregorio Antonny Bani*
Faculty of Science and Agriculture, Aryasatya Deo Muri University, Kupang, Indonesia

Mario Donald Bani
Department of Biotechnology, Indonesia International Institute for Life Sciences, East Jakarta, Indonesia

* Corresponding author. E-mail: greg.antonny@yahoo.com

Abstract
Plastic waste has many complex chemical components. In developing countries, direct incineration is often used to reduce plastic waste, releasing pollutants into the atmosphere. A more environmentally sound alternative is pyrolysis. It can turn plastic waste into an alternative fuel. A catalyst, such as natural zeolite, can reduce the energy used in pyrolysis. However, mineral contaminants must be removed first to get optimum activity. This research was focused on using Ende natural zeolite as a catalyst, determining the properties of the mineral in its activated form. It also investigated the interaction between H-zeolite composition and the operating temperature towards pyrolysis oil yield. The experimental results showed that Ende natural zeolite contained a mixture of mordenite, clinoptilolite, and quartz. After activation and modification, there was an increase in the surface area from 53.17–104.67 m^2/g. The average pore radius ranged from 19.96–34.21 Å. There was an increase in the pore volume from 22.01–72.34 cc/g. The total acidity changed from 1.456–5.342 NH$_3$/g. The optimum catalyst concentration was 10% in the pyrolysis of 1000 grams of plastic waste catalyzed by 100 grams of H-zeolite. The oil yield decreased at 15% concentration. The 10% concentration worked best at 400 °C.

Keywords: Catalyst, Plastic waste, Pyrolysis, Waste management, Zeolite

1 Introduction

Plastic is one of the most commonly used materials in the modern world due to its strength, lightweight, and versatility [1]. It is also cheap and more economical when producing plastic material in large quantities [2], leading to an accumulation of plastic trash. Polyethylene plastic is one of the most frequently used plastics for bags and packaging [3], [4]. The common chemical properties of polyethylene and other types of plastic include their high molecular weight with many aromatic rings and intricate chemical connections [5]. This chemical complexity does not allow plastic to be decomposed by microorganisms in the soil, leading to an accumulation of plastic cover that clogs the soil pores and pollutes the environment [6]. Many recycling methods have been developed to overcome the increased plastic waste [7]. However, it can only be carried out on specific types of waste in small quantities, and the remains still accumulate in landfills [8], [9].

In many developing countries, direct incineration is often preferred to reduce plastic waste because it is considered efficient and feasible [10]. However, this method releases pollutants into the air, such as volatile organic compounds (VOCs), NO$_X$, SO$_X$, CO, CO$_2$, polychlorinated dibenzofurans (PCDFs), and dioxins [11]. A more environmentally sound alternative to direct incineration is pyrolysis [12]. This thermal processing method employs high temperatures in a closed system, producing smaller chemical fractions as liquid fuel from plastic polymers without releasing

dangerous chemicals into the atmosphere [13], [14]. Pyrolysis requires a catalyst to help distribute products and efficiently use the energy [15], [16]. Zeolite is one of the best catalysts for pyrolysis [17], [18]. Zeolite is a porous, highly acidic mineral that can control the dispersion of pyrolysis fluids due to its high reactivity [19], [20]. Today, the best catalytic performance in pyrolysis is shown by synthetic zeolite, which is expensive and challenging to obtain [21].

Natural zeolite can be used as a cheap and more abundantly available alternative to synthetic zeolite [22]. This mineral can be found in almost all parts of Indonesia [23], including in the Ende District of Flores Island in East Nusa Tenggara Province [24]. Natural zeolite, which is predominantly found in the Indonesian archipelago, contains mordenite and clinoptilolite crystalline components, which have been known to have good resilience to high temperatures so that they can be employed as catalysts in pyrolysis [25]–[27]. However, in general, natural zeolite often displays very varied properties. The natural form tends to have different degrees of crystallinity, grade, pore size, and surface area. It reduces their catalytic performance, prevents their application as a catalyst in large-scale industries, and undermines their potential application [27]–[31].

For optimum catalytic performance, natural zeolite must first be activated and modified [32]. These procedures can remove impurities and improve natural zeolite's crystal structure, allowing better catalytic activity and providing the industry with cheaper catalysts from nature [33]. Several studies on modified natural zeolite from the Indonesian archipelago have confirmed this [34]. For example, after being activated with acid, Sukabumi natural zeolite converted 80% of the total styrofoam samples into oil yield that contained kerosene [35]. Another example, at 450 °C, Aceh natural zeolite, used as a catalyst in the pyrolysis of polypropylene plastic waste, produced 65% liquid from its total solid feedstock, with a gasoline composition of up to 96.71% [36]. In another study, as much as 90% of the polypropylene plastic was converted into pyrolysis oil, mostly gasoline components, using Klaten natural zeolite as the catalyst at 450 °C [37].

The oil produced by pyrolysis with plastics directly correlates to the type of plastic feedstock used in the reaction [38]. For example, only 60–80% of polyethylene plastic feedstock could be converted into pyrolysis oil [39]. On the other hand, up to 80–95% of polypropylene plastic could be converted into oil [40]. Other than this, in terms of utilizing natural zeolite as a catalyst in pyrolysis, the catalytic performance of natural zeolite is highly dependent on its natural properties [41]. These properties are directly linked to the location where the zeolite originates and the geological process that contributed to the formation of this mineral [42].

The diversity in natural zeolite properties does not allow similar activation and modification procedures for all natural zeolites [42]. The zeolite minerals from western Indonesia may have completely different natural features from those in the eastern region [25], [43], [44]. There have not been enough studies to generate sufficient information about the catalytic performance of natural zeolites originating from the eastern region of Indonesia, particularly from the Ende regency on Flores Island. This study generated data that added to the library of information about the catalytic activity of natural zeolite from eastern Indonesia, continuing our previous preliminary study on Ende natural zeolite [27]. The results of this study could determine the stability of Ende natural zeolite at the operating temperature of pyrolysis employed for polyethylene plastic waste.

2 Research Method

2.1 *Preparation of catalyst from ende natural zeolite*

The natural zeolite was taken from Ondorea village, on the southern coast of Ende district, Flores Island, Indonesia. The crushed Ende natural zeolite was put through a sieve with a mesh size of 100. The resulting zeolite powder was washed with water and then dried for 12 h at 120 °C in an oven to remove any leftover water and organic contaminants not washed away by water. This natural zeolite powder was then used to acquire the initial data for the catalyst, including the type of crystal components, surface morphology, surface area, pore radius, pore volume, and acidity.

The natural zeolite powder was activated by soaking it in a 1:2 (w/v) 1% hydrofluoric acid (HF) solution for 30 minutes, dissolving away more organic and inorganic contaminants. In this process, the silica

(Si) atoms on the mineral's outer framework should have interacted with fluorine [24], forming SiF_4 that would have dissolved away in the solution [43]. The pellet produced in this step was then dried for 24 h at 120 °C in an oven. After this step, the natural zeolite was called active Ende natural zeolite. An X-ray diffraction (XRD) analysis was used to characterize the dry powder produced from this step to understand how the activation procedure affected the crystallinity of its active form.

The active Ende natural zeolite powder was refluxed in a 6 M hydrochloric acid (HCl) solution by constantly stirring the slurry at 90 °C for 30 min to allow dealumination [44]. After decanting the liquid, the remaining pellet was rewashed with distilled water and dried at 130 °C for 3 h. The dried sample was then impregnated by refluxing it in a 1 M ammonium chloride (NH_4Cl) solution for seven days. During this period, the incubated slurry was stored in an oven, preventing any interaction with the atmosphere. Daily, the slurry was heated for 3 h at 90 °C. The continuous stirring and mixing allowed an interaction between active Ende natural zeolite and NH_4Cl. The slurry was filtered and dried at 130 °C for 3 h on the final day. Ammonium ions (NH_4^+) from the NH_4Cl solution were expected to replace the cations (e.g., Na^+ and Ca^{2+}) in the zeolite's framework [24], [45], [46].

The resulting dried powder after impregnation was then called active Ende H-zeolite. The residual ammonia (NH_3) in the zeolite's framework was cleaned through calcination at 500 °C for 2 h. Nitrogen gas was allowed to circulate to open up the pores in the zeolite's framework [24]. Several characterization methods were employed to reveal any changes in the active Ende H-zeolite.

2.2 Plastic waste preparation

The plastic waste used in this study was strictly taken from unused plastic containers with a polyethylene (PE) symbol. The PE plastic waste was then divided into small pieces of 0.5 × 0.5 cm [47]. For pyrolysis, 1000 grams of the small PE plastic pieces were used. Four different temperature treatments (300, 350, 400 and 450 °C) [48] were employed with four different catalyst compositions (0, 5, 10, and 15%) [47]. There were three technical replications in the experiment.

2.3 Pyrolysis of the plastic sample

There were 1000 grams of PE plastic pieces fed into the pyrolysis reactor for a reaction at 300 °C. A stopwatch was used to time the duration of pyrolysis. When the first pyrolysis oil drop came out of the reactor, it marked the initial time of the cracking process. At an interval of ten minutes, the oil reservoir was changed, and the oil volume was calculated. When no oil drop came out of the reactor anymore, the pyrolysis process was assumed to be completed, marking the end of the cracking process. A similar procedure was performed at 350, 400, and 450 °C [45]. For this first set of treatments, no catalyst was used.

The plastic waste and the active Ende H-zeolite were used in a ratio of 5% - where 50 grams of zeolite for every 1000 grams of plastic was used. This process was catalyst-induced pyrolysis conducted at 300 °C. The same procedure as the no-catalyst treatment was conducted here. When no oil drop was produced by the reactor anymore, the reaction was assumed to have ended. This catalyst-induced reaction was also performed at 350, 400, and 450 °C. Similar temperature treatments were also performed for the catalyst-to-feed concentrations of 10% and 15% [49].

2.4 Characterisation of zeolite as a catalyst

The characterization data included crystallinity components, surface area, and acidity. An X-ray diffractometer with an observation area between 10–90 degrees was used to determine the crystallinity components. The peak values of 2θ displayed in the diffractogram produced by the samples were qualitatively compared to the standard zeolite diffractogram of the International Centre for Diffraction Data [50]. The I/II percentage and the intensity produced by each sample were calculated by dividing the XRD experimental value for each sample by the value displayed in the standard diffractogram [34].

A scanning electron microscope (SEM) investigated the surface morphology. A gas sorption analyzer employing the Brunauer-Emmett-Teller method determined the surface area, pore radius, and pore volume. A gravimetric approach determined the acidity of the zeolite sample.

2.5 *Data analysis*

A randomized factorial design with two randomized elements was employed in this study. The first element was pyrolysis temperature with four levels: T_1, T_2, T_3, and T_4. The second element was catalyst and plastic waste, which had four levels: C_0, C_1, C_2, and C_3. Three repeats for each treatment were used. The mathematical model of the design was:

$$Y_{ij} = \mu + T_i + C_j + TC_{ij} + R_k + \epsilon_{ijk}$$

Y_{ij} : the observation results for the addition of the catalyst j at temperature i and repetition k
μ : the average
T_i : temperature i
C_j : catalyst j
TC_{ij} : the interaction between temperature i and catalyst j
R_k : repetition k
ϵ_{ijk} : possible measurement error at temperature i, for catalyst j at repetition k

Microsoft Excel 2007, Design Expert, and SPSS (Statistical Product and Service Solution) 23 were used to statistically process the experimental data generated by pyrolysis from each treatment. A regression analysis was used to process the cracking time ($ln\ k$) and the operating temperature of pyrolysis ($1/T$). These data were employed in the Arrhenius equation (Equations (1) and (2)) to calculate the activation energy for each catalyst increment.

$$k = k_0 exp(-A_e/RT) \tag{1}$$

k : the reaction rate constant (min^{-1})
k_0 : pre-exponential factor (min^{-1}) (independent of temperature)
A_e : activation energy (cal/mol)
T : absolute temperature of the reactor (K)
R : gas constant (1.986 cal/mol K).

By changing Equation (1) above to its logarithmic form, we get Equation (2) below:

$$ln\ k = ln\ k_0 - \left[\frac{A_e}{R}\right]\frac{1}{T} \tag{2}$$

If $Y = a + bX$,
      $Y = ln\ k$

$$b = (-A_e/R)$$
$$A_e = b.R$$
$$k_0 = exp\ (a)$$

The effects of each temperature level and the catalyst composition level were analyzed with a Response Surface Method (RSM). The RSM could better display the effects of interaction between different independent variables measured in the reaction towards the dependent variables. Based on the MANOVA acquired from RSM, the Least Significant Difference (LSD) test was performed on the dependent variables that showed significant differences. The LSD was performed to determine which independent variable had the most significant effects (the temperature, the catalyst, or their interaction) on the pyrolysis cracking time, volume, and oil yield.

3 Result and Discussion

3.1 *The zeolite characterization*

Ende natural zeolite is a bluish-colored mineral found in marine rocks in the southern coastal region of Flores Island, Indonesia. The color of natural zeolite highly depends on the type and amount of impurity adsorbed in its crystal structure [51]. It also depends on environmental conditions [33] and will significantly affect its properties and catalytic performance [52].

The 1% HF solution activation on Ende natural zeolite turned the color paler. This color change may have indicated that the impurities and the silica atoms in the outer framework of this mineral had dissolved into the acid solution [43]. This process rearranged the external framework of Ende natural zeolite, leaving more aluminum atoms that could be further removed and rearranged [24]. The dealumination of Ende natural zeolite with HCl ionized the abundantly available aluminum atoms into Al^{3+} cations and pulled more atoms from the inner framework into the outer one [53].

HCl reflux and heat treatment at 90 °C allowed the crystalline water molecules to get mixed with the acid solution and evaporate, providing a larger pore volume that aided in rearranging the atom positions within the zeolite framework [45]. In this process, the clear HCl solution turned greenish-yellow, indicating that the impurities had dissolved. The physical appearance
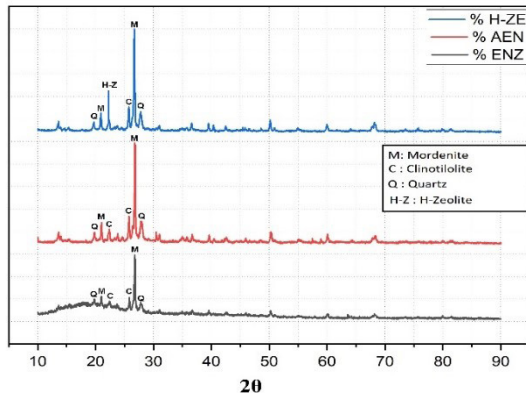
Figure 1: The diffractogram of Ende natural zeolite, active Ende natural zeolite, and active Ende H-zeolite.

of the active natural zeolite was pale white (Figure 1). Seven days of continuous washing and stirring of the active Ende natural zeolite in NH$_4$Cl solution allowed the release of the Cl$^-$ anions, leaving behind NH$_4^+$ cations and providing more H$^+$ to the zeolite [24], [46]. The treatment with NH$_4$Cl solution turned the color of the powder into pure white, indicating that the natural zeolite had changed to an active Ende H-Zeolite.

The characterization with XRD generated detailed information regarding the activation process. Figure 1 shows the results of the XRD analysis on Ende natural zeolite (bottom brown line), active Ende natural zeolite (middle red line), and active Ende H-Zeolite (top blue line). In Figure 1, the crystal intensity of the zeolite sample appears better when the crystalline water content inside the crystal packing has been removed [54]. The peaks of the crystal components appear taller and narrower in active Ende natural zeolite and active Ende H-Zeolite (see the red and blue lines in Figure 1), indicating the successful removal of water molecules and other impurities.

Our XRD analysis revealed that Ende natural zeolite has a particular crystal blend that consists of clinoptilolite and mordenite, consistent with the results from previous research [24], [27], [55]. The highest diffraction peak in Figure 1 corresponds to the mordenite crystal component, marked at $2\theta = 26.72°$ with a degree of crystallinity of 39.30%. The mordenite peak also appears at $2\theta = 22.26°$ with a 4.10% degree of crystallinity. The second highest component is the clinoptilolite crystal component, which peaks at $2\theta = 22.14°$ with 2.13% degree of

crystallinity and $2\theta = 26.68°$ with 5.69% degree of crystallinity.

Other than those two major crystal components, Figure 1 also shows a peak for the quartz crystal component that appears at $2\theta = 26.82°$ and $2\theta = 19.78°$ with 3.93% and 1.43% degree of crystallinity, respectively. Figure 1 also reveals many amorphous phase impurities from Ende natural zeolite that appear as a hill [56] in the brown bottom line generated by the sample before activation and modification. The many natural impurities in Ende natural zeolite may directly link to the fact that Flores Island belongs to the Ring of Fire with different active volcanoes [57]. The lava from these volcanoes might have immediately discharged into the sea, forcing too rapid cooling that eventually formed the natural zeolite. This rapid cooling process did not allow good packing of the atoms in the framework of the zeolite, leaving the atoms that do not occupy their lattice locations properly [58], [59].

After activation with HF solution, an amorphous line no longer appears in the diffractogram produced by the active Ende natural zeolite sample. Moreover, the mordenite peak at $2\theta = 26.78°$ increases its degree of crystallinity to 71.76%. The modernite peak at $2\theta = 22.28°$ also increases its degree of crystallinity to 7.23%. An increase in the degree of crystallinity to 9.11% and 3.45% can also be observed on the clinoptilolite peak that appears at $2\theta = 26.70°$ and $2\theta = 22.16°$, respectively. This activation procedure also increases the degree of crystallinity for the quartz peak at $2\theta = 26.84°$ (increases to 8.32%) and $2\theta = 19.80°$ (increases to 2.45%). The overall results of the XRD analysis concluded a successful activation procedure that only altered the chemical compositions of the natural zeolite without changing any of the main components.

The dealumination with HCl solution was used to eliminate some aluminum atoms from the framework of active Ende natural zeolite [60]. After that, the impregnation of H$^+$, accommodated by NH$_4$Cl solution, was carried out to compensate for the cation deficiency within the cavity [61]. This process was followed by calcination at 500 °C to increase the number of acid sites in the framework by dissociating NH$_3$ from NH$_4^+$, leaving behind H$^+$ cations in the zeolite cavity [45]. The use of nitrogen gas (N$_2$) in the calcination was meant to push out more impurities from the pores

and to expansively stretch the pores, making it easier for polyethylene hydrocarbon molecules to enter the cavities during the pyrolysis [24], [46]. The XRD results show that the H^+ impregnation was successful. As seen in Figure 1, the former peak corresponding to the clinoptilolite crystal component at $2\theta = 22.18°$ increases the degree of crystallinity to 12.56%. The increasing peak now corresponds to the H-Z component in the active Ende H-zeolite (see the top blue line).

In general, the impregnation results can be significantly affected by the overall surface morphology in the zeolite structure [62]. A non-uniform surface morphology at a molecular level creates a difference in the contact time between the zeolite's surface and the compound used for impregnation, in this case, NH_4Cl. This condition only allows the impregnation process to penetrate the surface with earlier contact with the NH_4Cl solution, producing non-uniform dispersion of the H^+ cations within the zeolite's framework [61]. The surface with earlier contact with the impregnating compound may have a higher accumulation of H^+ compared to the ones further away that have later contact [55]. Figure 2 shows the surface observation results using SEM. Before activation, the surface of Ende natural zeolite exhibited brittle, amorphous characteristics common in natural zeolite (Figure 2(a)). The zeolite's surface and pores were still covered in microscopic lumps of impurities. Following the activation procedure, the SEM revealed a more visible microstructure that better represented a composition of modernite. It can also be seen that there was less lump of impurities that covered the pore cavities with a concentrated H^+ dispersion (indicated by white colored region [61]) that is visible in a certain region only at the surface of the active Ende natural zeolite (Figure 2(b)) and active Ende H-zeolite (Figure 2(c)).

The ammonium deionization treatment for the active Ende natural zeolite rearranged its internal framework. This process provided more hydrogen ions (H^+) occupying the environment aluminum left behind. The SEM analysis confirmed that this process was successful. As seen in Figure 2(c), the cavities within the zeolite's framework are more uniform than those in Figures 2(a) and (b). However, Figure 2(c) also shows that the sample's surface after the impregnation does not appear as a well-uniformed morphology often displayed by a synthetic zeolite. As explained before,
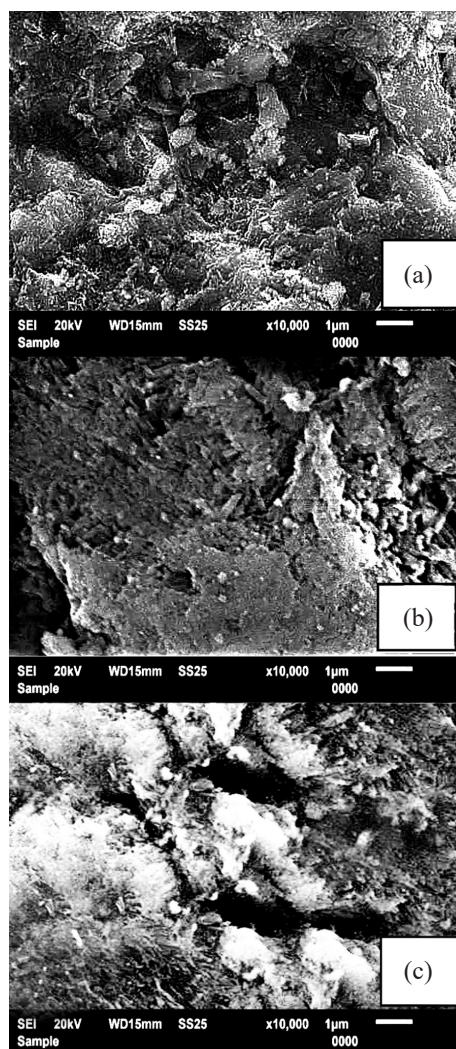

Figure 2: The SEM analysis results for the surface of Ende natural zeolite (a), active Ende natural zeolite (b), and the active Ende H-Zeolite (c).

the impregnated H^+ cations only got concentrated in a specific location on the surface of the active H-zeolite's framework. The polycrystalline morphology of a natural zeolite contributed to this by allowing the top layer to have a higher probability of adsorbing H^+ cations [55].

The non-uniformed surface morphology of natural zeolite may also affect its catalytic activity by not allowing a well-spread contact with the reactants. In a non-uniformed surface, the reactants may contact the catalyst faster in a spot closer to the reactants,
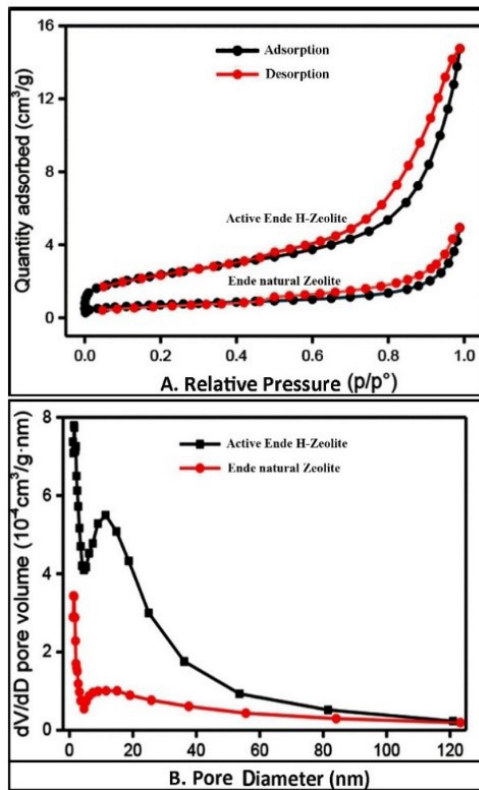
Figure 3: The results of the Brunauer-Emmett-Teller method for Ende natural zeolite before and after activation.

allowing a more prolonged contact and extended reaction. On another spot, further from the reactants, the contact occurs a bit later. Due to this uneven contact distribution, the overall reaction requires higher activation energy with a longer reaction time, producing poor-quality pyrolysis oil [63]. Modification and impregnation on a natural zeolite can produce an active zeolite form with a more even surface morphology. Although not as good as a synthetic zeolite, the more even surface morphology in active H-zeolite allows faster contact with the reactants, leading to better reactions with lower activation energy, producing good-quality pyrolysis oil [48].

Figure 3 shows the results of the Gas Sorption Analyzer, which employed the Brunauer-Emmett-Teller method, and it can be linked to Table 1. Figure 3 shows that the surface area, pore radius average, and pore volume increased in the active Ende H-zeolite. These data indicated an expansion of the pores on

the surface area of the zeolite after the activation and impregnation treatment. Based on the IUPAC classification of adsorption isotherms, Figure 3 shows that the relative pressure graph generated by Ende natural zeolite corresponds to the non-porous material type. This result is consistent with the SEM analysis shown in Figure 2(a), where clogging from different natural components was still visible on the sample's surface. After activation and impregnation, the sample's surface changed into a porous type with a non-uniform pore distribution. As seen in Figure 3(a), the hysteresis loop for the non-uniformed pores started at around $p/p° \approx 0.5$. The pore increase in active Ende H-zeolite was attributed to the contaminants that had dissolved in the HF, HCl and NH_4Cl solutions, opening up the pores within the framework. The impregnation of H^+ into the framework also increased the acidity of the zeolite, boosting its reactivity as a catalyst [61]. The active Ende H-zeolite also appeared to have increased the total acid sites.

Table 1: The analysis results of surface area, average pore radius, pore volume, and total acidity

Type	Surface Area (m²/g)	Average Pore Radius (Å)	Pore Volume (cc/g)	Acidity (mmol NH_3/g zeolite)
Natural Zeolite	53.17	19.96	22.01	1.456
H-Zeolite	104.67	34.21	72.34	5.342

3.2 *Activation energy*

Figure 4 shows the effect of different active Ende H-zeolite percentages as a catalyst towards the activation energy in the pyrolysis. Without a catalyst (0%), the pyrolysis showed almost 15,000 cal/mol of activation energy and a rate constant of 99,309.85 min⁻¹ for all temperature treatments. When the reaction was introduced with 5% of the catalyst, the activation energy was reduced by almost 1,600 cal/mol, and the reaction constant decreased by 43,259.81 min⁻¹. The pyrolysis with a 10% catalyst appeared to get a reduction of roughly 4,400 cal/mol with a reaction constant of 10,121.33 min⁻¹. However, when the catalyst was increased to 15%, the pyrolysis could only get a 3,000 cal/mol reduction in activation energy with a reaction constant of 58,629.9 min⁻¹, performing worse than the 10% catalyst.
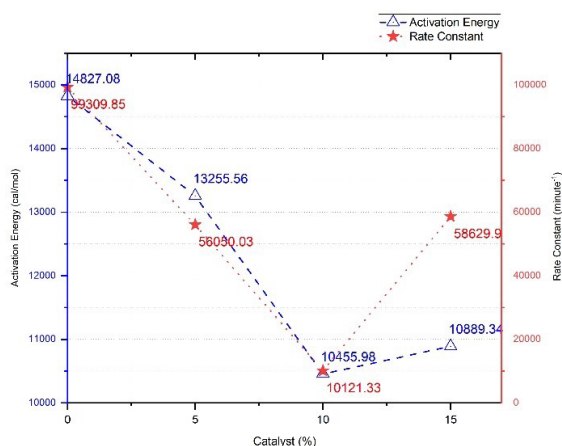
Figure 4: The activation energy in the pyrolysis with different catalyst percentages.

Figure 5: The effect of temperature and catalyst interaction on the pyrolysis time.

The 15% catalyst showed an inhibitory effect on the reaction. A catalyst in pyrolysis accommodates the breakdown of long hydrocarbon chains from polyethylene plastic waste into shorter chains. When the catalyst concentration is too high, insufficient substrate can be broken down into shorter chains. Moreover, pyrolysis may yield far too short gaseous hydrocarbons at high temperatures. The gaseous hydrocarbons can prevent the interaction between the active site within the zeolite framework and the substrates, gradually reducing its catalytic activity [64], [65].

3.3 *Pyrolysis oil yield*

Figure 5 shows the RSM results corresponding to the interaction between the observed reaction time, temperature treatments, and catalyst percentages. As shown in Figure 5, the reaction time would be faster with increasing temperature and catalyst percentage. At the highest temperature, 450 °C, the pyrolysis without catalyst completed the oil production in roughly 65 min. Adding 5, 10, and 15% of the catalyst completed the oil production in 40, 20, and 15 min, respectively. On the other hand, at the lowest temperature, 300 °C, the pyrolysis without a catalyst completed the oil production in 125 min. In contrast, adding 5, 10, and 15% of the catalyst completed the oil production in 108, 85, and 63 min, respectively.

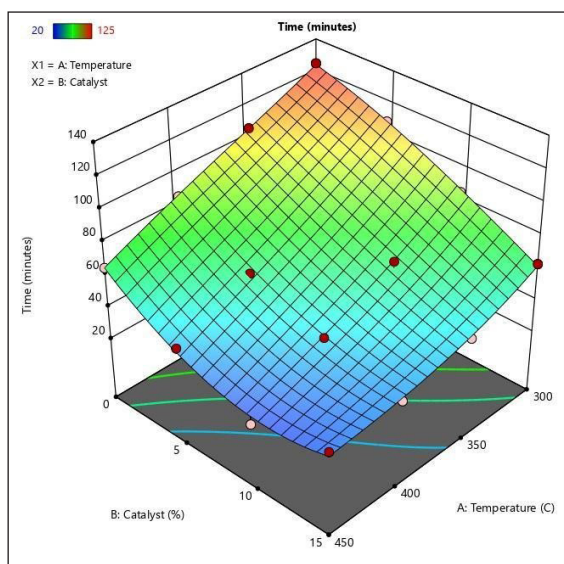The MANOVA analysis against temperature treatments, catalyst percentages, and the interaction between temperature and the catalyst showed a significant difference in the pyrolysis time (sig. = 0.000 < α = 0.001). The LSD test, performed against the temperature increase and the interaction between the temperature and the catalyst, also showed a significant difference in the pyrolysis time (sig. = 0.000 < α = 0.001). The LSD test also revealed that there was no significant difference between 10% and 15% treatment (sig. = 0.011 > α = 0.001).

Based on Figure 6, the volume of pyrolysis oil increased when there was an increase in the temperature and the catalyst percentage. However, the LSD test revealed that at 300 °C, there was no significant effect on the volume of pyrolysis oil (sig. = 0.05 > α = 0.001). This experimental result confirmed that the pyrolysis for polyethylene plastic is best carried out at temperatures above 300 °C, yielding the optimum volume of pyrolysis oil [66]. Other studies [67], [68] were consistent with this result, where the best pyrolysis temperature was above 450 °C. In this experiment, active Ende H-zeolite could reduce the pyrolysis temperature to 400 °C.

Although there was a significant difference between all temperature treatments, the LSD test did not show any significant difference between 10 and 15% catalyst percentage against the volume of pyrolysis oil (sig. = 0.02 > α = 0.01). The interaction
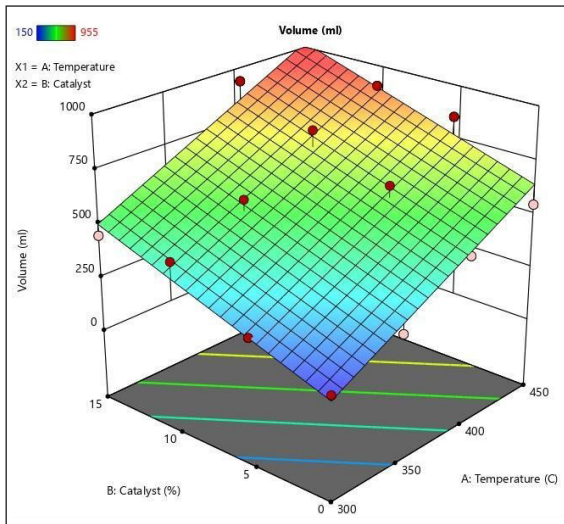
Figure 6: The effect of temperature and catalyst interactions on the volume of pyrolysis oil.

between the temperature and the catalyst percentage also showed a significant difference between 5% and 10% (sig. = 0.000 < α = 0.001), but not with 15% at all temperature treatments (sig. = 0.751 > α = 0.01).

3.4 *Pyrolysis oil characterization*

Figure 7 shows the quality test results for the pyrolysis oil. The increase in catalyst percentage and the temperature affected the viscosity of the pyrolysis oil. At 400 °C [Figure 7(a)], the reaction with 10% catalyst produced oil with a visible viscosity comparable to gasoline (ASTM 445). The oil viscosity became lower as the pyrolysis temperature increased. The LSD test revealed significant differences for all the treatments in the experiment (sig. = 0.000 < α = 0.001). However, to utilize the pyrolysis oil as fuel, 10% of active Ende H-zeolite at 400 °C appeared to be the best treatment, producing pyrolysis oil with similar traits to gasoline.

Other than viscosity, density is another important trait of pyrolysis oil that must be considered if it is to be used as fuel. The density of gasoline is around 0.7429 g/ml (ASTM D4502). In general, the viscosity of pyrolysis oil is directly proportional to its density - a decrease in viscosity also decreases the oil density. Figure 7(b) indicates that starting from 400 °C with 5% active Ende H-zeolite, the density of the pyrolysis oil matched the density of gasoline. The LSD test revealed
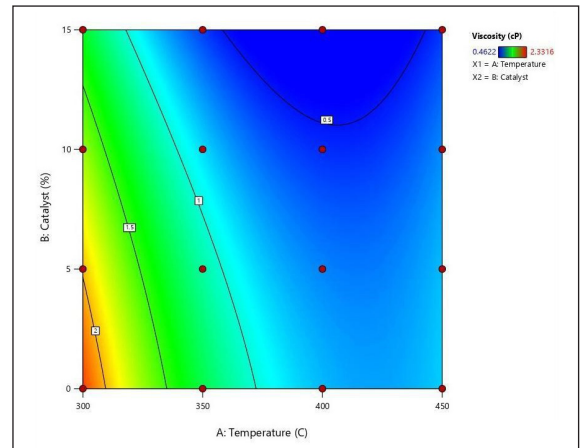
(a) Viscosity (cP)
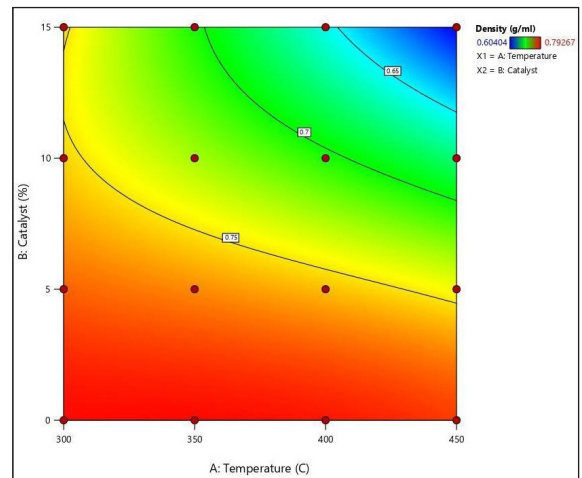
(b) Density (g/ml)

Figure 7: The results of the quality test for the pyrolysis oil.

that all the treatments and the interaction between the temperatures and the catalyst percentages were significantly different in lowering the oil density (sig. = 0.000 < α = 0.001).

The RSM result displayed in Figure 8 shows that different temperature treatments did not have any significant effects on the formation of C_5–C_{12} fractions (gasoline) in the pyrolysis oil (sig. = 0.002 > α = 0.001). The LSD test for each temperature treatment (with or without a catalyst) did not have any significant difference between 300 and 350 °C (sig. = 0.027 > α = 0.001). A similar pattern was also shown at 400 and 450 °C, with no significant difference (sig. = 0.364 >
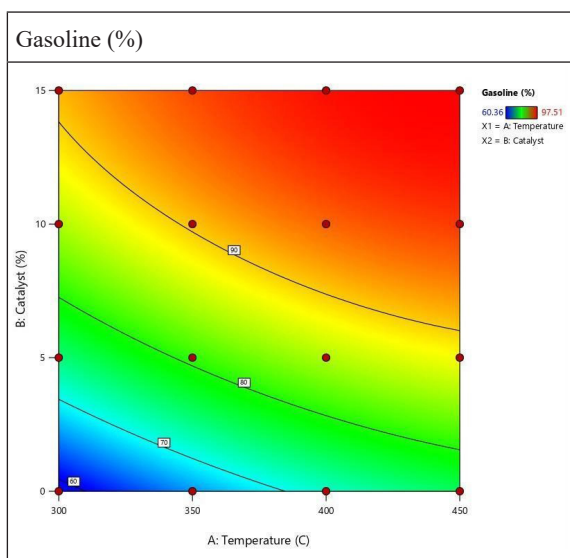
Figure 8: The gasoline percentage (C_5–C_{12} fractions) observed in the pyrolysis oil.

$\alpha = 0.001$) between these two treatments. However, the 300 ℃ treatment was significantly different from 400 ℃ (sig. = 0.001 ≤ α = 0.001) and 450 ℃ (sig. = 0.000 < α = 0.001). The same significant difference could also be observed from the 350 ℃ treatment when it was compared to 400 ℃ (sig. = 0.074 > α = 0.001) and 450 ℃ (sig. = 0.016 > α = 0.001).

These results indicated that it was unnecessary to continue the LSD test for the interaction between the temperatures and the catalyst percentages. It could be assumed that the temperature treatments did not do anything to the formation of the C_5–C_{12} fraction (gasoline). Temperature only accommodates the random breakdown of the long hydrocarbon chains of the polyethylene plastic, whereas zeolite as the catalyst directs the product's formation and distribution, eventually yielding a C_5–C_{12} fraction [37].

On the other hand, the RSM result in Figure 8 indicates obvious significant differences between the catalyst percentages (sig. = 0.000 < α = 0.001). A further LSD test showed that the percentage treatment was significantly different between 0%, 5%, and 10% (sig. = 0.000 < α = 0.001). No significant difference existed between 10% and 15% (sig. = 0.454 > α = 0.001). These results indicated that the 10% active Ende H-zeolite appeared to be the best composition to produce gasoline fractions in the pyrolysis of polyethylene plastic.

The catalytic activity of zeolite is due to active site pockets within the framework, allowing a quicker product formation [48]. Although important, high temperature does not directly impact the formation of the gasoline fractions that appear in the pyrolysis oil [68]. The experimental results in this study generally showed that only a small concentration of gasoline fractions could be generated by the reaction without H-zeolite as the catalyst. Adding 5%–10% significantly increased the gasoline fractions, yielding more oil products that can be distilled and utilized as fuel.

4 Conclusions

The natural zeolite collected from the southern coast of Flores mostly consists of mordenite, clinoptilolite, and quartz crystal components. The XRD analyses for the Ende natural zeolite before and after activation revealed a change in the degree of crystallinity without changing its main crystal component. This study revealed a change in the surface morphology due to a successful activation and modification of Ende natural zeolite. The surface area increased after impregnating H^+ cations, from 53.17–104.67 m^2/g. An increase was also observed in the average pore radius, from 19.96–34.21 Å. The pore volume increased from 22.01–72.34 cc/g. The value of the total acidity changed from 1.456–5.342 NH_3/g. The experimental results of this study indicated that 10% of active Ende H-zeolite as a catalyst in the pyrolysis at 400 ℃ had the best interaction in lowering the activation energy from 14,827–10,455 cal/mol. The 10 and 400 ℃ interaction also improved the rate constant of the reaction, the volume, and the quality of the pyrolysis oil.

Author Contributions

G.A.B.: came up with the main idea of the research, conducted the experiment, and wrote the manuscript; M.D.B.: contributed to the writing process, data analysis, and the overall development of the manuscript. Both authors contributed equally to this paper. They have read and approved the final version of the article.

Conflicts of Interest

The authors declare no conflict of interest.

References

[1] C. Wang, Y. Liu, W.-Q. Chen, B. Zhu, S. Qu, and M. Xu, "Critical review of global plastics stock and flow data," *Journal of Industrial Ecology*, vol. 25, no. 5, pp. 1300–1317, Oct. 2021, doi: 10.1111/jiec.13125.

[2] R. Karasik, N. E. Lauer, A. E. Baker, N. E Lisi, J. A. Somarelli, W. C. Eward, K. Fürst, and M. M. Dunphy-Daly, "Inequitable distribution of plastic benefits and burdens on economies and public health," *Frontiers in Marine Science*, vol. 9, pp. 1–11, Jan. 2023, doi: 10.3389/fmars.2022.1017247.

[3] J. J. Klemeš, Y. Van Fan, R. R. Tan, and P. Jiang, "Minimising the present and future plastic waste, energy and environmental footprints related to COVID-19," *Renewable and Sustainable Energy Reviews*, vol. 127, p. 109883, 2020, doi: 10.1016/j.rser.2020.109883.

[4] A. D. Sakti, A. N. Rinasti, E. Agustina, H. DIastomo, F. Muhammad, Z. Anna, and K. Wikantika, "Multi-scenario model of plastic waste accumulation potential in Indonesia using integrated remote sensing, statistic and socio-demographic data," *ISPRS International Journal of Geo-Information*, vol. 10, no. 7, 2021, doi: 10.3390/ijgi10070481.

[5] N. L. Bhandari, G. Bhandari, S. Bista, B. Pokhrel, K. Bist, and K. N. Dhakal, "Degradation of fundamental polymers/plastics used in daily life: A review," *Bibechana*, vol. 18, no. 1, pp. 240–253, 2021, doi: 10.3126/bibechana.v18i1.29619.

[6] M. G. Kibria, N. I. Masuk, R. Safayet, H. Q. Nguyen, and M. Mourshed, "Plastic waste: Challenges and opportunities to mitigate pollution and effective management," *International Journal of Environmental Research*, vol. 17, no. 1. 2023. doi: 10.1007/s41742-023-00507-z.

[7] S. Huang, H. Wang, W. Ahmad, A. Ahmad, N. I. Vatin, A. M. Mohamed, A. F. Deifalla, and I. Mehmood, "Plastic waste management strategies and their environmental aspects: A scientometric analysis and comprehensive review," *International Journal of Environmental Research and Public Health*, vol. 19, no. 8, 2022. doi: 10.3390/ijerph19084556.

[8] L. Traven and M. Široka, "Collection of recyclable waste in the city of Rijeka: Current status and perspectives, cleaner waste systems," *International Journal of Environmental Research and Public Health*, vol. 5, 2023, Art. no. 100093, doi: 10.1016/j.clwas.2023.100093.

[9] I. Wojnowska-Baryła, K. Bernat, and M. Zaborowska, "Plastic waste degradation in landfill conditions: The problem with microplastics, and their direct and indirect environmental effects," *International Journal of Environmental Research and Public Health*, vol. 19, no. 20, 2022, doi: 10.3390/ijerph192013223.

[10] C. A. Velis and E. Cook, "Mismanagement of plastic waste through open burning with emphasis on the global south: A systematic review of risks to occupational and public health," *Environmental Science and Technology*, vol. 55, no. 11, pp. 7186–7207, 2021, doi: 10.1021/acs.est.0c08536.

[11] P. Stegmann, V. Daioglou, M. Londo, D. P. van Vuuren, and M. Junginger, "Plastic futures and their CO_2 emissions," *Nature*, vol. 612, no. 7939, pp. 272–276, 2022, doi: 10.1038/s41586-022-05422-5.

[12] S. Armenise, W. SyieLuing, J. M. Ramírez-Velásques, F. Launay, D. Wuebben, N. Ngadi, J. Rams, and M. Muñoz, "Plastic waste recycling via pyrolysis: A bibliometric survey and literature review," *Journal of Analytical and Applied Pyrolysis*, vol. 158, 2021, doi: 10.1016/j.jaap.2021.105265.

[13] V. L. Mangesh, S. Padmanabhan, P. Tamizhdurai, and A. Ramesh, "Experimental investigation to identify the type of waste plastic pyrolysis oil suitable for conversion to diesel engine fuel," *Journal of Cleaner Production*, vol. 246, 2020, Art. no. 119066, doi: 10.1016/j.jclepro.2019.119066.

[14] F. Faisal, M. G. Rasul, M. I. Jahirul, and A. Ahmed, "Science of the total environment waste plastics pyrolytic oil is a source of diesel fuel: A recent review on diesel engine performance, emissions, and combustion characteristics," *Science of the Total Environment*, vol. 886, no. 2022, 2023, Art. no. 163756, doi: 10.1016/j.scitotenv.2023.163756.

[15] S. Maithomklang, K. Wathakit, E. Sukjit, B. Sawatmongkhon, and J. Srisertpol, "Utilizing

waste plastic bottle-based pyrolysis oil as an alternative fuel," *ACS Omega*, vol. 7, no. 24, pp. 20542–20555, 2022, doi: 10.1021/acsomega.1c07345.

[16] J. Liang, G. Shan, and Y. Sun, "Catalytic fast pyrolysis of lignocellulosic biomass: Critical role of zeolite catalysts," *Renewable and Sustainable Energy Reviews*, vol. 139, 2021, Art. no. 110707, doi: 10.1016/j.rser.2021.110707.

[17] R. Cai, X. Pei, H. Pan, H. Wan, H. Chen, Z. Huan, Z. Zhuo, and Y. Zhang, "Biomass catalytic pyrolysis over zeolite catalysts with an emphasis on porosity and acidity: A state-of-the-art review," *Energy & Fuels*, vol. 34, no. 10, pp. 11771–11790, Oct. 2020, doi: 10.1021/acs.energyfuels.0c02147.

[18] M. Abbas-abadi, Y. Ureel, A. Eschenbacher, F. H. Vermeire, R. John, J. Oenema, G. D. Stefanidis, and K. M. Van Geem, "Challenges and opportunities of light olefin production via thermal and catalytic pyrolysis of end-of-life polyolefins: Towards full recyclability," *Progress in Energy and Combustion Science*, vol. 96, 2023, Art. no. 101046, doi: 10.1016/j.pecs.2022.101046.

[19] H. Yuan, C. Li, R. Shan, J. Zhang, Y. Wu, and Y. Chen, "Recent developments on the zeolites catalyzed polyolefin plastics pyrolysis," *Fuel Processing Technology*, vol. 238, 2022, Art. no.107531, doi: 10.1016/j.fuproc.2022.107531.

[20] A. Marcilla, D. Berenguer, and I. Martinez, "Effect of the addition of zeolites and silicate compounds on the composition of the smoke generated in the decomposition of Heet tobacco under inert and oxidative atmospheres," *Journal of Analytical and Applied Pyrolysis*, vol. 164, 2022, Art. no. 105532, doi: 10.1016/j.jaap.2022.105532.

[21] M. Król, "Natural vs. Synthetic Zeolites," *Crystals*, vol. 10, no. 622, pp. 1–8, 2020, doi: 622; doi:10.3390/cryst10070622w.

[22] L. T. N. Maleiva, C. W. Purnomo, P. W. Nugraheni, E. Kusumawardhani, and L. S. A. Putra, "Zeolite effect on solid product characteristics in hydrothermal treatment of household waste," *ASEAN Journal of Chemical Engineering*, vol. 23, no. 1, pp. 52–61, 2023, doi: 10.22146/ajche.77544.

[23] D. D. Anggoro, I. Sumantri, and L. Buchori, "Indonesia's natural zeolite as an adsorbent for toxic gases in shrimp ponds," *Journal of Ecological Engineering*, vol. 22, no. 6, pp. 202–208, 2021, doi: 10.12911/22998993/137921.

[24] Y. A. B. Neolaka, Y. Lawa, J. Naat, A. A. P. Riwu, A. W. Mango, H. Darmokoesoemo, B. A. Widyaningrum, M. Iqbal, H. S. Kusuma, "Efficiency of activated natural zeolite-based magnetic composite (ANZ-Fe$_3$O$_4$) as a novel adsorbent for removal of Cr(VI) from wastewater," *Journal of Materials Research and Technology*, vol. 18, pp. 2896–2909, 2022, doi: 10.1016/j.jmrt.2022.03.153.

[25] D. Lestariningsih and T. Kurniawan, "Transformation of Natural Zeolites by the Fusion-Hydrothermal Method for Ammonium Adsorption," *World Chemical Engineering Journal*, vol. 7, no. 1, pp. 1–5, 2023.

[26] S. Narayanan, P. Tamizhdurai, V. L. Mangesh, C. Ragupathi, P. Santhana krishnan, and A. Ramesh, "Recent advances in the synthesis and applications of mordenite zeolite - review," *RSC Advances*, vol. 11, no. 1, pp. 250–267, 2020, doi: 10.1039/d0ra09434j.

[27] G. A. Bani, "Pemanfaatan zeolit alam Ende sebagai katalis dalam pirolisis polietilena dari sampah plastik," *Rekayasa Bahan Alam dan Energi Berkelanjutan*, vol. 07, no. 1, pp. 13–21, 2023.

[28] R. C. Ruiz-bastidas, G. Turnes, E. Palacio, and L. S. Cadavid-, "Natural Ecuadorian zeolite : An effective ammonia adsorbent to enhance methane production from swine waste," *Chemosphere*, vol. 336, 2023, Art. no. 139098, doi: 10.1016/j.chemosphere.2023.139098.

[29] A. N. An Naafi, R. T. Tjahjanto, and Y. P. Pranato, "Effect of NaOH concentration toward the characteristics of activated natural zeolite from blitar – east java," *Jurnal Kimia Sains dan Aplikasi*, vol. 26, no. 2, pp. 50–56, 2023, doi: 10.14710/jksa.26.2.50-56.

[30] L. F. De Magalhães, G. R. Da Silva, and A. E. C. Peres, "Zeolite application in wastewater treatment," *Adsorption Science and Technology*, vol. 2022, 2022, doi: 10.1155/2022/4544104.

[31] L. Velarde, M. Sadegh, E. Escalera, M. Antti, and F. Akhtar, "Adsorption of heavy metals on natural zeolites: A review," *Chemosphere*,

vol. 328, 2023, Art. no. 138508, doi: 10.1016/j.chemosphere.2023.138508.

[32] A. A. Vasconcelos, T. Len, A. de N. de Oliveira, A. A. F. da Costa, A. R. da Silva C. E. F da Costa, R. Luque, G. N. da Rocha Filho, R. C. R. Noronha L. A. S. do Nascimento, "Zeolites: a theoretical and practical approach with uses in (bio)chemical processes," *Applied Sciences (Switzerland)*, vol. 13, no. 3, 2023, doi: 10.3390/app13031897.

[33] E. Kuldeyev, M. Seitzhanova, S. Tanirbergenova, K. Tazhu, E. Doszhanov, Z. Mansurov, S. Azat, R. Nurlybaev, R. Berndtsson, "Modifying natural zeolites to improve heavy metal adsorption," *Water*, vol. 15, no. 12, p. 2215, 2023, doi: 10.3390/w15122215.

[34] J. Philia, W. Widayat, S. Sulardjaka, G. A. Nugroho, and A. N. Darydzaki, "Aluminum-based activation of natural zeolite for glycerol steam reforming," *Results in Engineering*, vol. 19, 2023, Art. no. 101247, doi: 10.1016/j.rineng.2023.101247.

[35] Suhartono, A. Romli, B. H. Prabowo, P. Kusumo, and Suharto, "Converting styrofoam waste into fuel using a sequential pyrolysis reactor and natural zeolite catalytic reformer," *International Journal of Technology*, vol. 14, no. 1, pp. 185–194, 2023, doi: 10.14716/ijtech.v14i1.4907.

[36] H. Husin, M. Mahidin, M. Marwan, and F. Nasution, "Conversion of polypropylene-derived crude pyrolytic oils using hydrothermal autoclave reactor and Ni / aceh natural zeolite as catalysts," *Heliyon*, vol. 9, no. 4, 2023, Art. no. e14880, doi: 10.1016/j.heliyon.2023.e14880.

[37] Nuryosuwito, S. Soeparman, W. Wijayanti, and N. Hamidi, "Natural zeolite study as a catalyst: A case study of pyrolysis of polyethene terephthalate (PET) waste into liquid fuel," *Journal of Physics: Conference Series*, vol. 1517, no. 1, 2020, doi: 10.1088/1742-6596/1517/1/012006.

[38] H. C. Genuino, M. Pilar Ruiz, H. J. Heeres, and S. R. A. Kersten, "Pyrolysis of mixed plastic waste: Predicting the product yields," *Waste Management*, vol. 156, no. 2022, pp. 208–215, 2023, doi: 10.1016/j.wasman.2022.11.040.

[39] M. I. Jahirul, F. Faisal, M. G. Rasul, D. Schaller, M. M. K. Khan, and R. B. Dexter, "Automobile fuels (diesel and petrol) from plastic pyrolysis oil—Production and characterisation," *Energy Reports*, vol. 8, pp. 730–735, 2022, doi: 10.1016/j.egyr.2022.10.218.

[40] M. M. Harussani, S. M. Sapuan, U. Rashid, A. Khalina, and R. A. Ilyas, "Pyrolysis of polypropylene plastic waste into carbonaceous char: Priority of plastic waste management amidst COVID-19 pandemic," *Science of the Total Environment*, vol. 803, p. 149911, 2022, doi: 10.1016/j.scitotenv.2021.149911.

[41] A. Irawan, T. Kurniawan, N. Nurkholifah, M. Melina, A. B. D. Nandiyanto, M. A. Firdaus, H. Alwan, Y. Bindar, "Pyrolysis of polyolefins into chemicals using low-cost natural zeolites," *Waste and Biomass Valorization*, vol. 14, no. 5, pp. 1705–1719, 2023, doi: 10.1007/s12649-022-01942-3.

[42] Ł. Kruszewski, V. Palchik, Y. Vapnik, K. Nowak, K. Banasik, and I. Galuskina, "Mineralogical, geochemical, and rock mechanic characteristics of zeolite-bearing rocks of the hatrurim basin, israel," *Minerals*, vol. 11, no. 10, 2021, doi: 10.3390/min11101062.

[43] S. Rojas-Buzo, P. Concepción, A. Corma, M. Moliner, and M. Boronat, "In-situ-generated active Hf-hydride in zeolites for the tandem N-alkylation of amines with benzyl alcohol," ACS Catalysis, vol. 11, no. 13, pp. 8049–8061, Jul. 2021, doi: 10.1021/acscatal.1c01739.

[44] P. Tobarameekul, S. Sangsuradet, N. N. Chat, and P. Worathanakul, "Enhancement of CO_2 adsorption containing zinc-ion-exchanged zeolite NaA synthesized from rice husk ash," *Applied Science and Engineering Progress*, vol. 15, no. 1, pp. 1–11, 2022, doi: 10.14416/j.asep.2020.11.006.

[45] H. Afriansyah, M. R. Ramlan, M. Roulina T, Y. Bow, and Fatria, "Pyrolysis of lubricant waste into liquid fuel using zeolite catalyst," *International Journal of Research in Vocational Studies (IJRVOCAS)*, vol. 1, no. 4, pp. 26–31, 2022, doi: 10.53893/ijrvocas.v1i4.72.

[46] A. Santoso, I. B. S. Sumari, N. N. Safitri, A. R. Wijaya, and D. E. K. Putri, "Activation of zeolite from malang as catalyst for plastic waste conversion to fuel," *Key Engineering Materials*, vol. 851, pp. 212–219, 2020, doi: 10.4028/www.

scientific.net/KEM.851.212.

[47] K. T. Kumaran and I. Sharma, "Catalytic pyrolysis of plastic waste: A review," *2020 Advances in Science and Engineering Technology International Conferences, ASET 2020*, vol. 2, pp. 822–838, 2020, doi: 10.1109/ ASET48392.2020.9118286.

[48] O. Y. Yansaneh and S. H. Zein, "Latest advances in waste plastic pyrolytic catalysis," *Processes*, vol. 10, no. 4, 2022, doi: 10.3390/pr10040683.

[49] O. A. Ogundele, A. Jimoh, and S. H. Paul, "Catalytic pyrolysis of polyethylene wastes into liquid fuel using ZSM-5 as catalyst," *International Journal of Scientific & Engineering Research*, vol. 10, no. 3, pp. 699–704, 2019.

[50] L. S. Campbell, J. Charnock, A. Dyer, S. Hillier, S. Chenery, F. Stoppa, C. M. B. Henderson, R. Walcott, M. Rumsey, "Determination of zeolite-group mineral compositions by electron probe microanalysis," *Mineralogical Magazine*, vol. 80, no. 5, pp. 781–807, 2016, doi: 10.1180/ minmag.2016.080.044.

[51] C. A. Ríos-reyes, G. A. Reyes-mendoza, J. A. Henao-martínez, C. Williams, and A. Dyer, "First report on the geologic occurrence of natural na–a zeolite and associated minerals in cretaceous mudstones of the paja formation of vélez (Santander), colombia," *Crystals*, vol. 11, no. 2, pp. 1–18, 2021, doi: 10.3390/cryst11020218.

[52] H. Zhang, I. bin Samsudin, S. Jaenicke, and G. K. Chuah, "Zeolites in catalysis: Sustainable synthesis and its impact on properties and applications," *Catalysis Science and Technology*, vol. 12, no. 19, pp. 6024–6039, 2022, doi: 10.1039/ d2cy01325h.

[53] I. M. R. Fattah, H. C. Ong, T. M. I. Mahlia, M. Mofijur, A. S. Silitonga, S. M. A. Rahman, A. Ahmad, "State of the art of catalysts for biodiesel production," *Frontiers in Energy Research*, vol. 851, pp. 1–17, 2020, doi: 10.3389/ fenrg.2020.00101.

[54] Y. Cheong, K. Wong, B. S. Ooi, T. C. Ling, and F. Khoerunnisa, "Behavior of K-MER zeolite and its morphological," *Crystals*, vol. 10, no. 64, pp. 1–15, 2020.

[55] S. Sugiarti, D. D. Septian, H. Maigita, N. A. Khoerunnisa, S. Hasanah, T. Wukirsari, N. Hanif, and Y. B. Aprilliyanto, "Investigation of H-zeolite and metal-impregnated zeolites as transformation catalysts of glucose to hydroxymethylfurfural," *AIP Conference Proceedings*, vol. 2243, no. 1, 2020.

[56] V. L. B. Fuss, G. Bruj, L. Dordai, M. Roman, O. Cadar, and A. Becze, "Evaluation of the impact of different natural zeolite treatments on the capacity of eliminating/reducing odors and toxic compounds," *Materials*, vol. 14, no. 13, 2021, doi: 10.3390/ma14133724.

[57] L. Spina, E. Del Bello, T. Ricci, J. Taddeucci, and P. Scarlato, "Multi-parametric characterization of explosive activity at Batu Tara Volcano (Flores Sea, Indonesia)," *Journal of Volcanology and Geothermal Research*, vol. 413, 2021, Art. no. 107199, doi: 10.1016/j.jvolgeores. 2021.107199.

[58] O. Cadar, M. Senila, M. A. Hoaghia, D. Scurtu, I. Miu, and E. A. Levei, "Effects of thermal treatment on natural clinoptilolite-rich zeolite behavior in simulated biological fluids," *Molecules*, vol. 25, no. 11, pp. 1–12, 2020, doi: 10.3390/molecules25112570.

[59] Z. Asgar Pour, Y. A. Alassmy, and K. O. Sebakhy, "A survey on zeolite synthesis and the crystallization process: Mechanism of nucleation and growth steps," *Crystals*, vol. 13, no. 6, pp. 1–13, 2023, doi: 10.3390/cryst13060959.

[60] L. L. Díaz-Muñoz, H. E. Reynel-Ávila, D. I. Mendoza-Castillo, A. Bonilla-Petriciolet, and J. Jáuregui-Rincón, "Preparation and characterization of alkaline and acidic heterogeneous carbon-based catalysts and their application in vegetable oil transesterification to obtain biodiesel," *International Journal of Chemical Engineering*, vol. 2022, 2022, doi: 10.1155/2022/7056220.

[61] Q. Zou, H. He, J. Xie, S. Han, W. Lin, A. K. Mondal, and F. Huang, "Study on the mechanism of acid modified H-Beta zeolite acidic sites on the catalytic pyrolysis of Kraft lignin," *Chemical Engineering Journal*, vol. 462, 2023, Art. no. 142029, doi: 10.1016/j.cej.2023.142029.

[62] V. Yadav, M. Rani, L. Kumar, N. Singh, and E. Varathan, "Effect of surface modification of natural zeolite on ammonium ion removal from water using batch study: An overview," *Water, Air, & Soil Pollution*, vol. 233, p. 465, Nov. 2022, doi: 10.1007/s11270-022-05948-4.

[63] P. Yan, I. N. Azreena, H. Peng, H. Rabiee, M. Ahmed, Y. Weng, Z. Zhu, E. M. Kennedy, and M. Stockenhuber, "Catalytic hydropyrolysis of biomass using natural zeolite-based catalysts," *Chemical Engineering Journal*, vol. 476, 2023, Art. no. 146630, doi: 10.1016/j.cej.2023.146630.

[64] V. Daligaux, R. Richard, and M. H. Manero, "Deactivation and regeneration of zeolite catalysts used in pyrolysis of plastic wastes—a process and analytical review," *Catalysts*, vol. 11, no. 7, 2021, doi: 10.3390/catal11070770.

[65] S. Xu, J. Chen, H. Peng, S. Leng, H. Li, W. Qu, Y. Hu, Hailong Li, S. Jiang, W. Zhou, L. Leng, "Effect of biomass type and pyrolysis temperature on nitrogen in biochar, and the comparison with hydrochar," *Fuel*, vol. 291, 2021, Art. no. 120128, doi: 10.1016/j.fuel.2021.120128.

[66] Sunaryo, Sutoyo, Suyitno, Z. Arifin, T. Kivevele, and A. I. Petrov, "Characteristics of briquettes from plastic pyrolysis by-products," *Mechanical Engineering for Society and Industry*, vol. 3, no. 2, pp. 57–65, 2023.

[67] S. H. Gebre, M. G. Sendeku, and M. Bahri, "Recent trends in the pyrolysis of non-degradable waste plastics," *ChemistryOpen*, vol. 10, no. 12, pp. 1202–1226, Dec. 2021, doi: 10.1002/open.202100184.

[68] W. Kaminsky, "Chemical recycling of plastics by fluidized bed pyrolysis," *Fuel Communications*, vol. 8, no. July, p. 100023, 2021, doi: 10.1016/j.jfueco.2021.100023.